

# Preparation for the Solar system observations with Herschel: Simulation of Jupiter observations with PACS

Hideo Sagawa<sup>\*,a</sup>, Paul Hartogh<sup>a</sup>, Miriam Rengel<sup>a</sup>, Arno de Lange<sup>b</sup>,  
Thibault Cavalie<sup>a</sup>

<sup>a</sup>*Max-Planck-Institut für Sonnensystemforschung, Max-Planck-str. 2, 37191 Katlenburg  
Lindau, Germany*

<sup>b</sup>*SRON Netherlands Institute for Space Research, Sorbonnelaan 2, 3584 CA Utrecht, The  
Netherlands*

---

## Abstract

Observations of the water inventory as well as other chemically important species on Jupiter will be performed in the frame of the guaranteed time key project of the Herschel Space Observatory entitled “*Water and related chemistry in the Solar system*”. Among other onboard instruments, PACS (Photodetector Array Camera and Spectrometer) will provide new data of the spectral atlas in a wide region covering the far-infrared and submillimetre domains, with an improved spectral resolution and a higher sensitivity compared to previous observations carried out by Cassini/CIRS (Composite InfraRed Spectrometer) and by ISO (Infrared Space Observatory).

In order to optimise the observational plan and to prepare for the data analysis, we have simulated the expected spectra of PACS Jupiter observations. Our simulation shows that PACS will promisingly detect several H<sub>2</sub>O emission lines. As PACS is capable of spatially resolving the Jovian disk,

---

\*Corresponding author. Tel.: +49 5556 979217, fax.: +49 5556 979240.

*Email address:* sagawa@linmpi.mpg.de (Hideo Sagawa)

we will be able to discern the external oxygen sources in the giant planets by exploring the horizontal distribution of water. In addition to H<sub>2</sub>O lines, some absorption lines due to tropospheric CH<sub>4</sub>, HD, PH<sub>3</sub> and NH<sub>3</sub> lines will be observed with PACS. Furthermore, owing to the high sensitivity of the instrument, the current upper limit on the abundance of hydrogen halides such as HCl will be also improved.

*Key words:* Jupiter, Planetary atmosphere, Remote sensing, Water vapour, PACS, Herschel Space Observatory, Far-infrared, Submillimetre, Spectrometre, Imager

---

## 1. Introduction

2 One of the most outstanding results in previous infrared observations of  
3 Jupiter is the detection of water in its stratosphere, achieved by ISO (In-  
4 frared Space Observatory) (Feuchtgruber et al., 1997; Lellouch et al., 1997).  
5 ISO has also detected CO<sub>2</sub> in the Jovian atmosphere (Lellouch et al., 2002)  
6 and these detections are regarded as a clear evidence for the existence of  
7 an external supply of oxygen into Jovian stratosphere. The observations  
8 of the Jovian water vapour with ISO have been followed by submillimetre  
9 (556.9 GHz) heterodyne observations by SWAS (the Submillimeter Wave As-  
10 tronomy Satellite) (Bergin et al., 2000; Lellouch et al., 2002) and the Odin  
11 satellite (Cavalié et al., 2008). In addition to monitoring the temporal vari-  
12 ability since the ISO observations, these spectrally resolved measurements  
13 constrained the vertical distribution of the Jovian stratospheric water vapour.  
14 Additional constraints on the possible external source have been obtained  
15 from the observations of CO, HCN and CS (e.g., Moreno et al., 2003; Griffith et al.,

16 2004). In the current picture, most of the exogenous species originate from  
17 the Shoemaker-Levy 9 (SL9) impacts in July 1994. However, other sources  
18 could be providers of oxygen, nitrogen and sulphur species as well in Jupiter  
19 as in the other giant planets. These potential sources are the following: i) the  
20 permanent interplanetary dust particle flux, ii) a local flux from the rings and  
21 icy moons via the magnetic field lines (Connerney, 1986), iii) sporadic large  
22 comet collision events. Discerning the relative contribution of each external  
23 source for each giant planet is a key issue, as it helps us in developing a full  
24 picture of various phenomena in the outer solar system such as the produc-  
25 tion of dust at large heliocentric distances, the role of the magnetosphere in  
26 the transport of exogenous material and the frequency of comet impacts.

27 The D/H ratio, which has been inferred from ISO measurements of the  
28 HD 37.7  $\mu\text{m}$  rotational line (Lellouch et al., 2001), is another key issue in  
29 Jovian atmospheric studies, because D/H on Jupiter and Saturn is considered  
30 as representative of the protosolar nebula while that on Uranus and Neptune  
31 represents the result of the mixing of the gases in the nebula with deuterium-  
32 rich icy cores (Feuchtgruber et al., 1999). Thus, the accurate comparison of  
33 D/H ratios on Jupiter and Saturn with Uranus and Neptune allows us to  
34 evaluate the D/H ratio of the protoplanetary ices embedded in the outer  
35 nebula, which is essential for a better understanding of the formation and  
36 evolution of the outer planets (Hersant et al., 2001).

37 These unsettled issues will be entirely re-addressed by new and sensi-  
38 tive observations that will be carried out with the Herschel Space Observa-  
39 tory (launched on 14 May 2009) which covers a wide spectral range in the  
40 far-infrared and submillimetre domains (approximately 55–672  $\mu\text{m}$ ). The

41 guaranteed time key programme “*Water and related chemistry in the so-*  
42 *lar system*” (Hartogh et al., 2009), also known as the HssO (Herschel Solar  
43 System Observations), is a dedicated project to observe water and other  
44 minor species in the solar system by using three onboard instruments: the  
45 Heterodyne Instrument for the Far Infrared (HIFI; de Graauw et al., 2008;  
46 de Graauw and 165 authors, 2010), the Spectral and Photometric Imaging  
47 REceiver (SPIRE; Griffin et al., 2008; Griffin and XX authors, 2010), and  
48 the Photodetector Array Camera and Spectrometer (PACS; Poglitsch et al.,  
49 2008; Poglitsch and XX authors, 2010). The focal plane units of these three  
50 instruments are kept cooled at the temperature range of 1.7–10 K by using  
51 superfluid helium, and the bolometric detectors of SPIRE and PACS are fur-  
52 ther cooled down to 0.3 K. As a result of this sophisticated active cooling sys-  
53 tem and also of the instrumental development such as the state-of-the-art SIS  
54 (superconductor-insulator-superconductor) mixers on HIFI, Herschel enables  
55 observing with a sensitivity that has never been achieved before. Among  
56 these instruments, PACS has the unique capability to obtain a spectral atlas  
57 in a wide wavelength range between 55 and 210  $\mu\text{m}$  with a resolving power of  
58 940–5500. This spectral resolution is rather low if compared to that of HIFI,  
59 and is not sufficient to resolve the molecular line shapes. However, our previ-  
60 ous preparatory study for the HssO Titan observations (Rengel et al., 2009)  
61 has demonstrated that PACS spectroscopic observations can be employed to  
62 retrieve the vertical temperature profile and constrain the  $\text{H}_2\text{O}$  abundance in  
63 Titan’s atmosphere by combining the observations of several lines of different  
64 opacity.

65 In this study, we intend to extend our simulation study to the Jupiter

66 observations. The Jupiter observations that are planned within the HssO  
67 project are described in Section 2. The method used for the simulation is  
68 presented in Section 3, and expected results of PACS spectroscopy on Jupiter  
69 are discussed in Section 4. The summary is given in Section 5.

## 70 **2. Planned Jupiter observations with Herschel**

71 Within the framework of the HssO project, PACS and HIFI are the pro-  
72 posed instruments for the Jupiter observations. SPIRE is not included in the  
73 proposal since its detector saturates when observing the bright continuum of  
74 Jupiter.

75 PACS will be used in its spectroscopy mode for the HssO Jupiter observa-  
76 tions. It is operated as an integral field spectrometer between 55 and 210  $\mu\text{m}$   
77 over a field-of-view (FOV) of  $47'' \times 47''$  (with a  $5 \times 5$  pixel array). The  $47''$  FOV  
78 is comparable to the apparent disk diameter of Jupiter in its visible windows  
79 ( $36\text{--}45''$ ), which enables us to obtain the disk resolved spectro-imaging of  
80 Jupiter with a single exposure. An image slicer is used to transform the sig-  
81 nal observed with  $5 \times 5$  spatial pixels (1 pixel corresponds to  $9.4''$ ) at the focal  
82 plane into  $1 \times 25$  pixels which is the entrance slit for the grating spectrom-  
83 eter. The grating is operated in its first ( $102\text{--}210 \mu\text{m}$ ), second ( $72\text{--}98 \mu\text{m}$ ),  
84 or third ( $55\text{--}72 \mu\text{m}$ ) order. Two photoconductor arrays ( $16 \times 25$  pixels, where  
85 16 pixels are for the spectral dimension and 25 for the spatial) of red ( $102\text{--}$   
86  $210 \mu\text{m}$ ) and blue ( $55\text{--}98 \mu\text{m}$ ) channels are operated simultaneously, therefore  
87 it is possible to observe two grating orders together, either combination of  
88  $1^{st} + 2^{nd}$  or  $1^{st} + 3^{rd}$ . The spectral resolving power varies in a range of 940–  
89 5500 depending on wavelength and grating order. The instantaneous spectral

90 coverage (for 16 pixels) also varies from  $\sim 0.15$  to  $1.05 \mu\text{m}$  as well.

91 Two observing modes, *line scan* and *range scan* modes, are prepared for  
92 the PACS spectroscopy. The line scan mode is employed when one observes  
93 one or several unresolved narrow line features in a fixed wavelength range  
94 of around  $1 \mu\text{m}$ , while the range scan mode is used to observe any wider  
95 wavelength range. High and low spectral sampling configurations are avail-  
96 able for these line and range scans. Molecular lines will be sampled with at  
97 least two spectral pixels even at the low sampling rate. PACS can obtain  
98 a full range spectrum between  $55$  and  $210 \mu\text{m}$  (so-called *SED* mode) in one  
99 hour by combining two low sampling range scans ( $\sim 1300$  seconds for observ-  
100 ing the  $55\text{--}73$  and  $102\text{--}146 \mu\text{m}$  ranges, and  $\sim 2400$  seconds for  $70\text{--}105$  and  
101  $140\text{--}210 \mu\text{m}$ ). The expected noise equivalent spectral radiance (NESR) for a  
102 single repetition of the SED range scan observation is  $0.8\text{--}4.0$  Jy varying as a  
103 function of the wavelength (the best sensitivity is achieved at the wavelength  
104 region of  $110\text{--}140 \mu\text{m}$ ). It is to be noted that this sensitivity estimation is  
105 valid when observing a low/moderate brightness source, and it is subject to  
106 change for the Jupiter observations which contain a very bright continuum  
107 emission. The optimization of the instrumental setup of PACS for the bright  
108 target is now under way by the PACS Instrument Control Centre. More  
109 details of the instrumental information can be found in the PACS observer's  
110 manual<sup>1</sup>.

111 The proposed Jupiter observations with PACS are:

- 112 • The high signal-to-noise ratio (SNR) *SED range scan* from  $55$  to  $210 \mu\text{m}$ ,

---

<sup>1</sup>[http://herschel.esac.esa.int/Docs/PACS/pdf/pacs\\_om.pdf](http://herschel.esac.esa.int/Docs/PACS/pdf/pacs_om.pdf)

113 which aims at not only the observation of numerous water lines but also  
114 the first detection of hitherto unobserved molecules. An SNR of at least  
115 100 with respect to the continuum is required in the HssO proposal.

- 116 • A dedicated *line scan* spectroscopy observation of the 66.4  $\mu\text{m}$  (4512 GHz)  
117  $\text{H}_2\text{O}$  line with the high spectral sampling mode.

118 In order to search for temporal variability, these observations (as well as the  
119 undermentioned HIFI observations except the mapping one) will be repeated  
120 three times during the lifetime of Herschel ( $\sim 3.5$  years).

121 As the explicit instrumental sensitivity of PACS for the very bright source  
122 is not confirmed yet, we do not have the practical number of the expected  
123 SNR for the abovementioned observation programmes. According to the re-  
124 cent results of the PACS Performance Verification phase, an SNR of at least  
125 1000 with respect to the continuum is currently expected for the Jupiter  
126 SED range scan observation (personal communications with Helmut Feucht-  
127 gruber). Instead, in this study we investigate the possible outcome of the  
128 PACS Jupiter observation for the SNR required in the guaranteed time pro-  
129 posal i.e. SNR  $>100$  with respect to the continuum.

130 Although the focus of the present study is the PACS observations, we  
131 briefly describe here about the Jupiter observations with HIFI in the HssO  
132 project as they provide essential information of the vertical profile of the wa-  
133 ter vapour. HIFI is composed of two HEB (hot electron bolometer) and five  
134 SIS mixer bands that cover the wavelength range of 157–212 and 240–625  $\mu\text{m}$   
135 (corresponding to 1910–1410 and 1250–480 GHz, respectively). As backends,  
136 two spectrometers are available; the High Resolution Spectrometer (HRS,  
137 an auto-correlator spectrometer) and the Wide Band Spectrometer (WBS,

138 an acousto-optical spectrometer). HRS enables the instantaneous coverage  
139 of 250 MHz with spectral resolutions ranging from 0.14 to 0.54 MHz, or cov-  
140 erage of 500 MHz with 1.1 MHz resolution, while WBS covers 4 GHz with a  
141 spectral resolution of 1.1 MHz. The beam size of HIFI is 11–44'' depending  
142 on the observing wavelength.

143 With HIFI, the following Jupiter observations are proposed:

- 144 • High SNR observations of the strong H<sub>2</sub>O lines at 557, 1097, and/or  
145 1670 GHz (538.2, 273.2 and/or 179.5 μm). From their line shapes, the  
146 vertical profile of H<sub>2</sub>O will be retrieved.
  
- 147 • Rough mapping (10 points over the Jovian disk) of the 1670 or 1717 GHz  
148 H<sub>2</sub>O line (the beam size of HIFI is ~12'' at these frequencies). Com-  
149 bined to the PACS observations, these observations will be used to  
150 determine the spatial distribution of H<sub>2</sub>O in the atmosphere of Jupiter.
  
- 151 • The 1882 GHz (159.3 μm) CH<sub>4</sub> line observation. CH<sub>4</sub> in Jupiter is con-  
152 sidered to be uniformly mixed in altitude and its abundance is well  
153 known. Therefore, its spectral line shape will provide us with the ther-  
154 mal profile.

### 155 3. Simulation of the PACS observations

156 Our simulation package is based on the general forward and inversion  
157 model called MOLIERE-v5 (Urban et al., 2004). The forward model consists  
158 of a radiative transfer model for the Jovian atmosphere and an instrumen-  
159 tal part where the atmospheric spectrum is convolved with Herschel's main  
160 beam pattern and PACS spectral response. We use a line-by-line radiative



161 transfer model with a multi-layered spherical atmosphere which the pres-  
162 sure levels ranging from 6 bar to  $2 \times 10^{-4}$  mbar. The reference temperature  
163 profile is based on the radio occultation experiments of Voyager 2 (Table 1  
164 in Lindal, 1992) and the *in situ* measurement of the Galileo entry probe  
165 (Seiff et al., 1998). For simplicity, we use a smoothed temperature profile  
166 for the stratosphere (Fig. 1(a)).  $\text{NH}_3$ ,  $\text{PH}_3$ ,  $\text{CH}_4$ ,  $\text{CO}$ ,  $\text{HCN}$ ,  $\text{H}_2\text{O}$ ,  $\text{HCl}$  and  
167  $\text{HD}$  are considered in the line opacity calculations. Adopted vertical pro-  
168 files of their mixing ratios are shown in Fig. 1(b). The profiles of  $\text{NH}_3$  and  
169  $\text{PH}_3$  are based on the reference model of Nixon et al. (2007). The  $\text{CH}_4$  pro-  
170 file is based on the photochemical model of Moses et al. (2005). Profiles of  
171  $\text{H}_2\text{O}$ ,  $\text{CO}$  and  $\text{HCN}$  are derived from the observations of the SL9 impact  
172 (Lellouch et al., 1997; Bézard et al., 2002; Moreno et al., 2003). For  $\text{HCl}$ ,  
173 an upper limit of 2.3 ppb has been retrieved from the Cassini/CIRS (Com-  
174 posite InfraRed Spectrometer) measurements (Fouchet et al., 2004). In this  
175 study, we use three  $\text{HCl}$  profiles having vertically constant mixing ratios of  
176 2.3, 1.15 and 0.23 ppb, respectively. The spectroscopic parameters are de-  
177 rived from the HITRAN 2008 compilation (Rothman et al., 2009) except for  
178  $\text{PH}_3$  and  $\text{HD}$ . Parameters for  $\text{PH}_3$  are derived from the GEISA 2003 com-  
179 pilation (Jacquinet-Husson et al., 2005). For  $\text{HD}$ , the parameters from the  
180 CDMS compilation (Müller et al., 2005) are used. We have used two line  
181 shape functions depending on the pressure: The Voigt line shape is used at  
182 the pressures where the pressure broadened half width is less than 40 times  
183 of the Doppler half width. At higher pressures, the Van Vleck-Weisskopf  
184 line shape is adopted alternatively. The pressure broadening line widths are  
185 derived from those listed in the HITRAN and GEISA databases which are

186 appropriate for the Earth atmosphere, because there are few laboratory and  
187 theoretical works on those induced by Hydrogen and Helium in particular at  
188 the submillimetre/far-infrared spectral region. The collision induced absorp-  
189 tion coefficients of H<sub>2</sub> and He mixtures are included by using the formulation  
190 of Borysow et al. (1985, 1988). Possible additional opacity due to clouds and  
191 hazes was not considered in this preparatory work. The distance between  
192 Herschel and Jupiter was set to 5 AU, corresponding to an apparent disk  
193 diameter of 39". We assume that the telescope is pointing to the centre of  
194 the disk, and calculate the spectrum detected by the central pixel of the  
195 PACS detector array. The radiative transfer calculation was performed with  
196 a very fine spectral grid, containing all the transition frequencies and the  
197 nearby line wing frequencies of the species mentioned previously, in order  
198 to evaluate the line shape of the molecular emission correctly. The synthe-  
199 sised spectrum after the radiative transfer calculation is convolved by the  
200 PACS instrumental function which accounts for its finite spectral resolution  
201 ( $\lambda/\Delta\lambda = 940\text{--}5500$ ). As described in the previous section, the spectral sam-  
202 plings (i.e. frequencies at the final spectral grid to be synthesised) of PACS  
203 vary depends on the observing mode. In order to examine the best possible  
204 performance of PACS full range scan observations, we used an oversampled  
205 spectral grid which includes all the molecular transition frequencies.

206 In this study, we simulate the PACS Jupiter spectrum with an SNR of  
207 100 with respect to the continuum emission at the reference wavelength of  
208 200  $\mu\text{m}$ . For other wavelengths, we scaled the corresponding NESR from the  
209 standard SED range scan observation in accordance with its frequency de-  
210 pendency. This assumed NESR results in the PACS Jupiter spectrum having

211 an SNR as high as  $\sim 1200$  with respect to the continuum at the wavelength  
212 around  $110\ \mu\text{m}$ , and lower than 100 at the end wavelengths of each grating  
213 order.

214 The sensitivity of PACS measurements to the atmospheric parameter of  
215 interest (such as the vertical distribution of  $\text{H}_2\text{O}$ ) is examined by calculating  
216 the weighting functions. The weighting function is defined as the derivative  
217 of the forward model with respect to the atmospheric parameter at each  
218 measurement frequency channel.

## 219 4. Expected outcome of PACS observations

### 220 4.1. $\text{H}_2\text{O}$ measurement with PACS

221 As previously described in Section 2, the primary objective of the HssO  
222 project with respect to Jupiter observations is to determine the vertical and  
223 horizontal distribution of water in the Jovian stratosphere. We therefore  
224 start with examining the sensitivity of PACS full range scan spectroscopy  
225 observations to the water vapour abundance.

226 Figures 2–3 show the synthetic full range spectra of Jupiter considering  
227 PACS spectral resolution. For comparison, the synthetic spectrum before  
228 convolution with the instrumental function is also shown there. The con-  
229 tinuum emission comes from the collision induced opacity of the  $\text{H}_2$  and He  
230 atmosphere, and the broad absorption line features of tropospheric  $\text{NH}_3$ . Al-  
231 though a large number of the roto-vibrational transitions of the considered  
232 species are present in the frequency region of interest (see ticks on the middle  
233 panels of Fig. 2–3), most of them are severely broadened due to PACS finite  
234 spectral resolution and become indistinctive from the continuum. However,

235 by checking the line-to-continuum ratio, a couple of molecular lines including  
236 H<sub>2</sub>O show their emission/absorption amplitude being as large as  $\sim 7\%$  of the  
237 continuum. Under the assumed NESR conditions (i.e. SNR of  $\sim 100$ – $1200$   
238 with respect to the continuum), those lines will certainly be detected from  
239 the set of PACS observations.

240 While ISO/LWS (Long Wavelength Spectrometer) observations have re-  
241 sulted in the detection of the two strongest H<sub>2</sub>O emission lines at 66.4 and  
242 99.5  $\mu\text{m}$  in the PACS spectral range, Cassini/CIRS has not succeeded in de-  
243 tecting any H<sub>2</sub>O line in the Jovian atmosphere due to the limitations in terms  
244 of spectral resolution and sensitivity. In case of the assumed PACS measure-  
245 ments with an SNR of 100 at 200  $\mu\text{m}$ , our calculations suggest that many  
246 more H<sub>2</sub>O lines, up to 22 in the presented case, become detectable at the  $5\text{-}\sigma$   
247 level for the first time in this far-infrared/submillimetre domain (indicated  
248 by arrows on the lowermost panels of Fig. 2–3).

249 Figure 4(a),(b) shows the weighting functions, with respect to the as-  
250 sumed H<sub>2</sub>O vertical profile, for the 66.4  $\mu\text{m}$  H<sub>2</sub>O line before and after consid-  
251 ering PACS spectral resolution, respectively. Although the 66.4  $\mu\text{m}$  line when  
252 computed at infinite spectral resolution show sensitivity to a wide altitude  
253 range, all the weighting functions show their peaks at the same pressure level  
254 of 10–20 mbar after smoothing to PACS spectral resolution. This is also the  
255 case for all other H<sub>2</sub>O transitions in the PACS spectrum (Fig. 4(c)). This  
256 means that we will be able to measure the H<sub>2</sub>O abundance in this single  
257 altitude layer from the PACS multiple line measurements. From the per-  
258 spective of exploring the vertical profile of H<sub>2</sub>O in the Jovian stratosphere,  
259 the observations planned with HIFI are required.

260 The most interesting Jovian water observation with PACS is the inves-  
261 tigation of a possible variation of its abundance as a function of latitude.  
262 Recent Cassini/CIRS observations have revealed that HCN and CO<sub>2</sub>, which  
263 were both injected by the SL9 impact, are distributed over the planet in quite  
264 different ways (Lellouch et al., 2006). Thus, it is of interest to investigate the  
265 latitudinal variations in the H<sub>2</sub>O field as probably most of the stratospheric  
266 water originates also from this impact (Lellouch et al., 2002; Cavalié et al.,  
267 2008). This observation is possible because of the 5×5 pixel coverage of  
268 PACS, and will be the first ever mapping of Jupiter at H<sub>2</sub>O frequencies.

#### 269 *4.2. Detectability of minor species*

270 In addition to H<sub>2</sub>O lines, several rotational lines of CH<sub>4</sub> are expected to  
271 be detected by PACS. In Jupiter, CH<sub>4</sub> is distributed almost uniformly in both  
272 the troposphere and stratosphere. Unlike HIFI, PACS is not sensitive to the  
273 narrow emission line of CH<sub>4</sub> coming from the stratosphere but will be able  
274 to observe accurately the absorption caused by tropospheric CH<sub>4</sub> (Fig. 5(a)).

275 For the currently undetected species, the detection or stringent con-  
276 straints on their abundances are expected with the PACS observations, since  
277 PACS achieves a higher spectral resolution and sensitivity than Cassini/CIRS.  
278 As an example, we present the detectability of HCl with PACS in this study.  
279 We have calculated the spectra for different mixing ratios; 2.3 ppb (current  
280 upper limit, and the spectra are shown in the Fig. 2–3), 1.15 ppb and 0.23 ppb.  
281 From the lowermost panels of Fig. 2–3, it is expected that the HCl(4–3)  
282 transition at 119.9 μm is observed with the highest SNR among other HCl  
283 transitions, and can be used for acquiring the lower upper limit on the HCl  
284 abundance. Even in the case of the lowest assumed abundance, the HCl(4–3)

285 spectral feature is likely observed at the  $5\text{-}\sigma$  level (Fig. 5(b)). HCl and other  
286 hydrogen halides are theoretically expected to condense into solid ammo-  
287 nium halide salts (e.g.,  $\text{NH}_4\text{Cl}$ ) around the cold Jovian upper troposphere;  
288 therefore, the hydrogen halide vapours may only be detectable if they are  
289 present at disequilibrium for any reason. PACS observations of the HCl and  
290 other hydrogen halide abundances will improve the thermochemical modeling  
291 including the  $\text{NH}_3$  cloud microphysics of Jupiter.

292 Fig. 5(c),(d) shows the synthetic spectra of HD rotational transitions R(0)  
293 and R(1) located at  $112.1$  and  $56.2\ \mu\text{m}$  ( $2675$  and  $5331$  GHz), respectively,  
294 assuming HD/ $\text{H}_2$  ratio of  $4.8\times 10^{-5}$  (Lellouch et al., 2001). Although the  
295 R(1) transition has a  $\sim 2.5$  times higher line opacity than R(0), the R(0)  
296 transition might be the best target for PACS to improve the accuracy of the  
297 previously measured HD/ $\text{H}_2$  ratios in the giant planets from the view point of  
298 the sensitivity of the PACS spectrometer. In fact, the HD R(0) transition lies  
299 at the most sensitive wavelength region of the PACS spectrometer, while the  
300 position of the R(1) line is very close to the end of PACS spectral range where  
301 its sensitivity substantially degrades. Moreover, the HD R(1) line in Jupiter  
302 is located in intense  $\text{NH}_3$  manifolds which makes difficult to determine the  
303 continuum level accurately (here continuum is referenced to the  $\text{H}_2$  and He  
304 collision induced absorptions and to the  $\text{NH}_3$  opacity). Under the assumed  
305 NESR conditions, the  $10\text{-}\sigma$  detection of the HD R(0) line is expected even  
306 though absorption depth is estimated as small as  $1\%$  of the continuum.

#### 307 *4.3. Sensitivity to tropospheric $\text{PH}_3$ and $\text{NH}_3$*

308 PACS will be sensitive to the  $\text{PH}_3$  abundance in the upper troposphere,  
309 from  $\sim 600$  mbar to  $80$  mbar (Fig. 6(a)).  $\text{PH}_3$ , particularly in the upper tro-

310 posphere, is considered to be an important probe for investigating the ver-  
311 tical and meridional atmospheric transport in the giant planets.  $\text{PH}_3$  is  
312 enriched in the upper troposphere with respect to predictions by thermo-  
313 dynamic equilibrium models. This has been interpreted as an evidence for  
314 rapid upward transportation of air from the deep interior as explained below  
315 (e.g., Barshay and Lewis, 1978).  $\text{PH}_3$  is convectively transported from the  
316 deep hot atmosphere into the upper troposphere where it is in disequilib-  
317 rium with the cold ambient temperatures. Because the equilibrium reaction  
318 ( $4\text{PH}_3 + 6\text{H}_2\text{O} \rightarrow \text{P}_4\text{O}_6 + 12\text{H}_2$ ) is very slow compared to the diffusion time  
319 scale,  $\text{PH}_3$  actually remains in disequilibrium leading to the observed en-  
320 hanced abundances.

321 Recent studies with Cassini/CIRS and ground-based telescopes observa-  
322 tions (Irwin et al., 2004; Fletcher et al., 2009a,b) have revealed an enhance-  
323 ment of the  $\text{PH}_3$  abundance at the equator compared to the neighbouring  
324 equatorial belts and mid-latitudes. Unfortunately, PACS spatial resolution  
325 is too low compared to the resolution of these previous observations so that  
326 PACS may not be able to observe such a fine latitudinal inhomogeneity;  
327 but still, PACS observations will be important in that they will extend the  
328 current results with a new observing wavelength region (currently,  $\text{PH}_3$  is in-  
329 vestigated using the CIRS spectra at mid-infrared  $1200\text{ cm}^{-1}$  region). This  
330 will confirm previous findings and/or lead to new insights.

331 Tropospheric  $\text{NH}_3$  will also be measured and, by analysing its very broad  
332 absorption lines, the bulk abundance of  $\text{NH}_3$  at the level from  $\sim 800$  mbar to  
333 100 mbar will be determined (Fig. 6(b)). This will improve our knowledge  
334 of the enrichment of nitrogen in Jupiter with respect to the solar value (Jo-

335 vian nitrogen is enriched by a factor of  $\sim 3$  with respect to the solar value,  
336 (Wong et al., 2004)) along with carbon and sulphur, which have been first  
337 confirmed by the Galileo probe measurements (Owen et al., 1999).

## 338 5. Summary

339 The Herschel Space Observatory will bring new insights into the origin of  
340 stratospheric water as well as other controversial issues in the Jovian atmo-  
341 sphere, in the frame of the guaranteed time key programme entitled “*Water*  
342 *and related chemistry in the Solar system*”.

343 To optimise the observational plan and to prepare for the data analysis,  
344 we have simulated the expected Jupiter spectra as observed with PACS in the  
345 full range scan mode by developing a forward model that takes into account  
346 the radiative transfer in the Jovian atmosphere and PACS instrumental char-  
347 acteristics. Several H<sub>2</sub>O emission lines will be detected for the first time in the  
348 wide far-infrared/submillimetre domains, and some absorption lines due to  
349 the tropospheric CH<sub>4</sub>, PH<sub>3</sub> and NH<sub>3</sub>. As PACS is capable of spatially resolv-  
350 ing Jupiter, we will be able to newly constrain the origin of water in Jupiter  
351 by determining its horizontal distribution. Furthermore, the constraints on  
352 the abundances of hydrogen halides such as HCl will be also improved with  
353 respect to the current upper limit derived from the Cassini/CIRS measure-  
354 ments. For the observation of HD with PACS, our simulations suggest its  
355 rotational transition R(0) as the possible target to observe by making effec-  
356 tive use of the most sensitive wavelength of the PACS spectrometer.



357 **References**

358 Barshay, S. S., Lewis, J. S., 1978. Chemical structure of the deep atmosphere  
359 of Jupiter. *Icarus* 33, 593–611.

360 Bergin, E. A., Lellouch, E., Harwit, M., Gurwell, M. A., Melnick, G. J.,  
361 Ashby, M. L. N., Chin, G., Erickson, N. R., Goldsmith, P. F., Howe,  
362 J. E., Kleiner, S. C., Koch, D. G., Neufeld, D. A., Patten, B. M., Plume,  
363 R., Schieder, R., Snell, R. L., Stauffer, J. R., Tolls, V., Wang, Z., Win-  
364 newisser, G., Zhang, Y. F., 2000. Submillimeter Wave Astronomy Satellite  
365 Observations of Jupiter and Saturn: Detection of 557 GHz Water Emis-  
366 sion from the Upper Atmosphere. *The Astrophysical Journal Letters* 539,  
367 L147–L150.

368 Bézard, B., Lellouch, E., Strobel, D., Maillard, J.-P., Drossart, P., 2002.  
369 Carbon Monoxide on Jupiter: Evidence for Both Internal and External  
370 Sources. *Icarus* 159, 95–111.

371 Borysow, J., Frommhold, L., Birnbaum, G., 1988. Collision-induced roto-  
372 translational absorption spectra of H<sub>2</sub>-He pairs at temperatures from 40  
373 to 3000 K. *The Astrophysical Journal* 326, 509–515.

374 Borysow, J., Trafton, L., Frommhold, L., Birnbaum, G., 1985. Modeling  
375 of pressure-induced far-infrared absorption spectra: Molecular hydrogen  
376 pairs. *The Astrophysical Journal* 296, 644–654.

377 Cavalié, T., Billebaud, F., Biver, N., Dobrijevic, M., Lellouch, E., Bril-  
378 let, J., Lecacheux, A., Hjalmarson, Å., Sandqvist, A., Frisk, U., Ol-  
379 berg, M., Bergin, E. A., The Odin Team, 2008. Observation of water

380 vapor in the stratosphere of Jupiter with the Odin space telescope. Plan-  
381 etary & Space Science 56, 1573–1584.

382 Connerney, J. E. P., 1986. Magnetic connection for Saturn’s rings and atmo-  
383 sphere. Geophysical Research Letters 13, 773–776.

384 de Graauw, T., 165 authors, 2010. The Herschel-Heterodyne Instrument for  
385 the Far-Infrared (HIFI). Astronomy & Astrophysics, in press.

386 de Graauw, T., Whyborn, N., Helmich, F., Dieleman, P., Roelfsema, P.,  
387 Caux, E., Phillips, T., Stutzki, J., Beintema, D., Benz, A., Biver, N.,  
388 Boogert, A., Boulanger, F., Cherednichenko, S., Coeur-Joly, O., Comito,  
389 C., Dartois, E., de Jonge, A., de Lange, G., Delorme, I., DiGiorgio, A.,  
390 Dubbeldam, L., Edwards, K., Fich, M., Güsten, R., Herpin, F., Honingh,  
391 N., Huisman, R., Jacobs, H., Jellema, W., Kawamura, J., Kester, D.,  
392 Klapwijk, T., Klein, T., Kooi, J., Krieg, J., Kramer, C., Kruizenga, B.,  
393 Laauwen, W., Larsson, B., Leinz, C., Liseau, R., Lord, S., Luinge, W.,  
394 Marston, A., Merkel, H., Moreno, R., Morris, P., Murphy, A., Naber, A.,  
395 Planesas, P., Martin-Pintado, J., Olberg, M., Orleanski, P., Ossenkopf,  
396 V., Pearson, J., Perault, M., Phillip, S., Rataj, M., Ravera, L., Saraceno,  
397 P., Schieder, R., Schmuelling, F., Szczerba, R., Shipman, R., Teyssier, D.,  
398 Vastel, C., Visser, H., Wildeman, K., Wafelbakker, K., Ward, J., Higgins,  
399 R., Aarts, H., Tielens, X., Zaal, P., 2008. The Herschel-Heterodyne Instru-  
400 ment for the Far-Infrared (HIFI): instrument and pre-launch testing. In:  
401 Society of Photo-Optical Instrumentation Engineers (SPIE) Conference  
402 Series. Vol. 7010 of Society of Photo-Optical Instrumentation Engineers  
403 (SPIE) Conference Series.

404 Feuchtgruber, H., Lellouch, E., Bézard, B., Encrenaz, T., de Graauw, T.,  
405 Davis, G. R., 1999. Detection of HD in the atmospheres of Uranus and  
406 Neptune: a new determination of the D/H ratio. *Astronomy & Astro-*  
407 *physics* 341, L17–L21.

408 Feuchtgruber, H., Lellouch, E., de Graauw, T., Bézard, B., Encrenaz, T.,  
409 Griffin, M., 1997. External supply of oxygen to the atmospheres of the  
410 giant planets. *Nature* 389, 159–162.

411 Fletcher, L. N., Orton, G. S., Teanby, N. A., Irwin, P. G. J., 2009a. Phosphine  
412 on Jupiter and Saturn from Cassini/CIRS. *Icarus* 202, 543–564.

413 Fletcher, L. N., Orton, G. S., Yanamandra-Fisher, P., Fisher, B. M., Parrish,  
414 P. D., Irwin, P. G. J., 2009b. Retrievals of atmospheric variables on the  
415 gas giants from ground-based mid-infrared imaging. *Icarus* 200, 154–175.

416 Fouchet, T., Orton, G., Irwin, P. G. J., Calcutt, S. B., Nixon, C. A., 2004.  
417 Upper limits on hydrogen halides in Jupiter from Cassini/CIRS observa-  
418 tions. *Icarus* 170, 237–241.

419 Griffin, M., Swinyard, B., Vigroux, L., Abergel, A., Ade, P., André, P., Ba-  
420 luteau, J., Bock, J., Franceschini, A., Gear, W., Glenn, J., Huang, M.,  
421 Griffin, D., King, K., Lellouch, E., Naylor, D., Oliver, S., Olofsson, G.,  
422 Perez-Fournon, I., Page, M., Rowan-Robinson, M., Saraceno, P., Sawyer,  
423 E., Wright, G., Zavagno, A., Abreu, A., Bendo, G., Dowell, A., Dowell, D.,  
424 Ferlet, M., Fulton, T., Hargrave, P., Laurent, G., Leeks, S., Lim, T., Lu,  
425 N., Nguyen, H., Pearce, A., Polehampton, E., Rizzo, D., Schulz, B., Sidher,  
426 S., Smith, D., Spencer, L., Valtchanov, I., Woodcraft, A., Xu, K., Zhang,

- 427 L., 2008. Herschel-SPIRE: design, ground test results, and predicted per-  
428 formance. In: Society of Photo-Optical Instrumentation Engineers (SPIE)  
429 Conference Series. Vol. 7010 of Society of Photo-Optical Instrumentation  
430 Engineers (SPIE) Conference Series.
- 431 Griffin, M. J., XX authors, 2010. The Herschel-SPIRE instrument and its  
432 in-flight performance. *Astronomy & Astrophysics*, in press.
- 433 Griffith, C. A., Bézard, B., Greathouse, T., Lellouch, E., Lacy, J., Kelly, D.,  
434 Richter, M. J., 2004. Meridional transport of HCN from SL9 impacts on  
435 Jupiter. *Icarus* 170, 58–69.
- 436 Hartogh, P., Lellouch, E., Crovisier, J., Banaszekiewicz, M., Bensch, F.,  
437 Bergin, E. A., Billebaud, F., Biver, N., Blake, G. A., Blecka, M. I., Blom-  
438 maert, J., Bockelée-Morvan, D., Cavalié, T., Cernicharo, J., Courtin, R.,  
439 Davis, G., Decin, L., Encrenaz, P., Encrenaz, T., González, A., de Graauw,  
440 T., Hutsémekers, D., Jarchow, C., Jehin, E., Kidgers, M., Küppers, M.,  
441 de Lange, A., Lara, L.-M., Lis, D. C., Lorente, R., Manfroid, J., Medvedev,  
442 A. S., Moreno, R., Naylor, D. A., Orton, G., Portyankina, G., Rengel, M.,  
443 Sagawa, H., Sánchez-Portal, M., Schieder, R., Sidher, S., Stam, D., Swin-  
444 yard, B., Szutowicz, S., Thomas, N., Thornhill, G., Vandenbussche, B.,  
445 Verdugo, E., Waelkens, C., Walker, H., 2009. Water and related chemistry  
446 in the solar system. a guaranteed time key program for herchel. *Plane-  
447 tary & Space Science* 57, 1596–1606.
- 448 Hersant, F., Gautier, D., Huré, J.-M., 2001. A Two-dimensional Model for  
449 the Primordial Nebula Constrained by D/H Measurements in the Solar

450 System: Implications for the Formation of Giant Planets. *The Astrophysical*  
451 *Journal* 554, 391–407.

452 Irwin, P. G. J., Parrish, P., Fouchet, T., Calcutt, S. B., Taylor, F. W.,  
453 Simon-Miller, A. A., Nixon, C. A., 2004. Retrievals of jovian tropospheric  
454 phosphine from Cassini/CIRS. *Icarus* 172, 37–49.

455 Jacquinet-Husson, N., Scott, N. A., Chédin, A., Garceran, K., Armante,  
456 R., Chursin, A. A., Barbe, A., Birk, M., Brown, L. R., Camy-Peyret,  
457 C., Claveau, C., Clerbaux, C., Coheur, P. F., Dana, V., Daumont, L.,  
458 Debacker-Barilly, M. R., Flaud, J. M., Goldman, A., Hamdouni, A., Hess,  
459 M., Jacquemart, D., Köpke, P., Mandin, J. Y., Massie, S., Mikhailenko,  
460 S., Nemtchinov, V., Nikitin, A., Newnham, D., Perrin, A., Perevalov,  
461 V. I., Régalia-Jarlot, L., Rublev, A., Schreier, F., Schult, I., Smith, K. M.,  
462 Tashkun, S. A., Teffo, J. L., Toth, R. A., Tyuterev, V. G., Vander Auwera,  
463 J., Varanasi, P., Wagner, G., 2005. The 2003 edition of the GEISA/IASI  
464 spectroscopic database. *Journal of Quantitative Spectroscopy and Radia-*  
465 *tive Transfer* 95, 429–467.

466 Lellouch, E., Bézard, B., Fouchet, T., Feuchtgruber, H., Encrenaz, T., de  
467 Graauw, T., 2001. The deuterium abundance in Jupiter and Saturn from  
468 ISO-SWS observations. *Astronomy & Astrophysics* 370, 610–622.

469 Lellouch, E., Bézard, B., Moses, J. I., Davis, G. R., Drossart, P., Feucht-  
470 gruber, H., Bergin, E. A., Moreno, R., Encrenaz, T., 2002. The Origin of  
471 Water Vapor and Carbon Dioxide in Jupiter’s Stratosphere. *Icarus* 159,  
472 112–131.

- 473 Lellouch, E., Bézard, B., Strobel, D. F., Bjoraker, G. L., Flasar, F. M.,  
474 Romani, P. N., 2006. On the HCN and CO<sub>2</sub> abundance and distribution  
475 in Jupiter's stratosphere. *Icarus* 184, 478–497.
- 476 Lellouch, E., Feuchtgruber, H., de Graauw, T., Encrenaz, T., Bézard,  
477 B., Griffin, M., 1997. Deuterium and Oxygen in Giant Planets. In:  
478 A. M. Heras, K. Leech, N. R. Trams, & M. Perry (Ed.), *The first ISO*  
479 *workshop on Analytical Spectroscopy*. Vol. 419 of ESA Special Publica-  
480 *tion*. pp. 131–135.
- 481 Lindal, G. F., 1992. The atmosphere of Neptune - an analysis of radio oc-  
482 *cultation data acquired with Voyager 2*. *The Astrophysical Journal* 103,  
483 967–982.
- 484 Moreno, R., Marten, A., Matthews, H. E., Biraud, Y., 2003. Long-term evolu-  
485 *tion of CO, CS and HCN in Jupiter after the impacts of comet Shoemaker-*  
486 *Levy 9*. *Planetary & Space Science* 51, 591–611.
- 487 Moses, J. I., Fouchet, T., Bézard, B., Gladstone, G. R., Lellouch, E., Feucht-  
488 *gruber, H., 2005. Photochemistry and diffusion in Jupiter's stratosphere:*  
489 *Constraints from ISO observations and comparisons with other giant plan-*  
490 *ets*. *Journal of Geophysical Research (Planets)* 110 (E9), 8001.
- 491 Müller, H. S. P., Schlöder, F., Stutzki, J., Winnewisser, G., 2005. The  
492 *Cologne Database for Molecular Spectroscopy, CDMS: a useful tool for*  
493 *astronomers and spectroscopists*. *Journal of Molecular Structure* 742, 215–  
494 227.

495 Niemann, H. B., Atreya, S. K., Carignan, G. R., Donahue, T. M., Haberman,  
496 J. A., Harpold, D. N., Hartle, R. E., Hunten, D. M., Kasprzak, W. T.,  
497 Mahaffy, P. R., Owen, T. C., Way, S. H., 1998. The composition of the  
498 Jovian atmosphere as determined by the Galileo probe mass spectrometer.  
499 *Journal of Geophysical Research (Planets)* 103, 22831–22846.

500 Nixon, C. A., Achterberg, R. K., Conrath, B. J., Irwin, P. G. J., Teanby,  
501 N. A., Fouchet, T., Parrish, P. D., Romani, P. N., Abbas, M., Leclair, A.,  
502 Strobel, D., Simon-Miller, A. A., Jennings, D. J., Flasar, F. M., Kunde,  
503 V. G., 2007. Meridional variations of C<sub>2</sub>H<sub>2</sub> and C<sub>2</sub>H<sub>6</sub> in Jupiter’s atmo-  
504 sphere from Cassini CIRS infrared spectra. *Icarus* 188, 47–71.

505 Owen, T., Mahaffy, P., Niemann, H. B., Atreya, S., Donahue, T., Bar-Nun,  
506 A., de Pater, I., 1999. A low-temperature origin for the planetesimals that  
507 formed Jupiter. *Nature* 402, 269–270.

508 Poglitsch, A., Waelkens, C., Bauer, O. H., Cepa, J., Feuchtgruber, H., Hen-  
509 ning, T., van Hoof, C., Kerschbaum, F., Krause, O., Renotte, E., Ro-  
510 driguez, L., Saraceno, P., Vandenbussche, B., 2008. The Photodetector  
511 Array Camera and Spectrometer (PACS) for the Herschel Space Obser-  
512 vatory. In: *Society of Photo-Optical Instrumentation Engineers (SPIE)*  
513 *Conference Series*. Vol. 7010 of *Society of Photo-Optical Instrumentation*  
514 *Engineers (SPIE) Conference Series*.

515 Poglitsch, A., XX authors, 2010. The Photodetector Array Camera and Spec-  
516 trometer (PACS) on the Herschel Space Observatory. *Astronomy & Astro-*  
517 *physics*, in press.

- 518 Rengel, M., Sagawa, H., Hartogh, P., 2009. Retrieval Simulation of Atmo-  
519 spheric Gases from Herschel observations of Titan. *Advances in Geoscience*  
520 in press.
- 521 Rothman, L. S., Gordon, I. E., Barbe, A., Benner, D. C., Bernath, P. F.,  
522 Birk, M., Boudon, V., Brown, L. R., Campargue, A., Champion, J.-P.,  
523 Chance, K., Coudert, L. H., Dana, V., Devi, V. M., Fally, S., Flaud, J.-  
524 M., Gamache, R. R., Goldman, A., Jacquemart, D., Kleiner, I., Lacome,  
525 N., Lafferty, W. J., Mandin, J.-Y., Massie, S. T., Mikhailenko, S. N.,  
526 Miller, C. E., Moazzen-Ahmadi, N., Naumenko, O. V., Nikitin, A. V., Or-  
527 phal, J., Perevalov, V. I., Perrin, A., Predoi-Cross, A., Rinsland, C. P.,  
528 Rotger, M., Šimečková, M., Smith, M. A. H., Sung, K., Tashkun, S. A.,  
529 Tennyson, J., Toth, R. A., Vandaele, A. C., Vander Auwera, J., 2009.  
530 The HITRAN 2008 molecular spectroscopic database. *Journal of Quanti-*  
531 *tative Spectroscopy and Radiative Transfer* 110, 533–572.
- 532 Seiff, A., Kirk, D. B., Knight, T. C. D., Young, R. E., Mihalov, J. D., Young,  
533 L. A., Milos, F. S., Schubert, G., Blanchard, R. C., Atkinson, D., 1998.  
534 Thermal structure of Jupiter’s atmosphere near the edge of a 5- $\mu\text{m}$  hot spot  
535 in the north equatorial belt. *Journal of Geophysical Research (Planets)* 103,  
536 22857–22890.
- 537 Urban, J., Baron, P., Lauté, N., Schneider, N., Dassas, K., Ricaud, P., de  
538 La Noë, J., 2004. Moliere (v5): a versatile forward- and inversion model  
539 for the millimeter and sub-millimeter wavelength range. *Journal of Quan-*  
540 *titative Spectroscopy and Radiative Transfer* 83, 529–554.
- 541 Wong, M. H., Mahaffy, P. R., Atreya, S. K., Niemann, H. B., Owen, T. C.,



542 2004. Updated Galileo probe mass spectrometer measurements of carbon,  
543 oxygen, nitrogen, and sulfur on Jupiter. *Icarus* 171, 153–170.

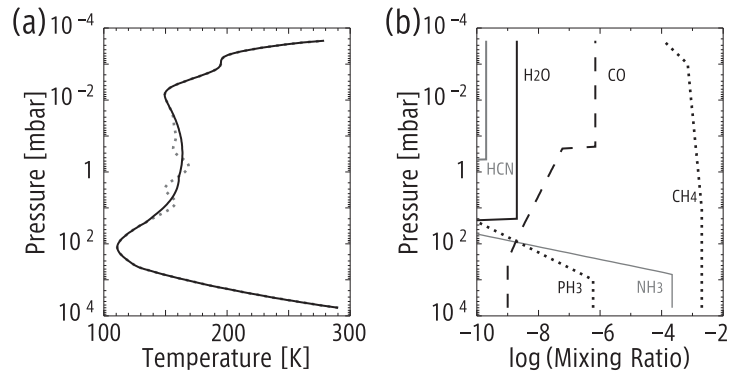


Figure 1: (a) Temperature and (b) molecular mixing ratio profiles used in this study. The dotted temperature profile represents the result obtained by the Galileo entry probe (Seiff et al., 1998). The mole fractions of  $\text{H}_2$  and He are set to 0.863 and 0.134, respectively, as measured by the Galileo probe (Niemann et al., 1998) and not shown in the plot.

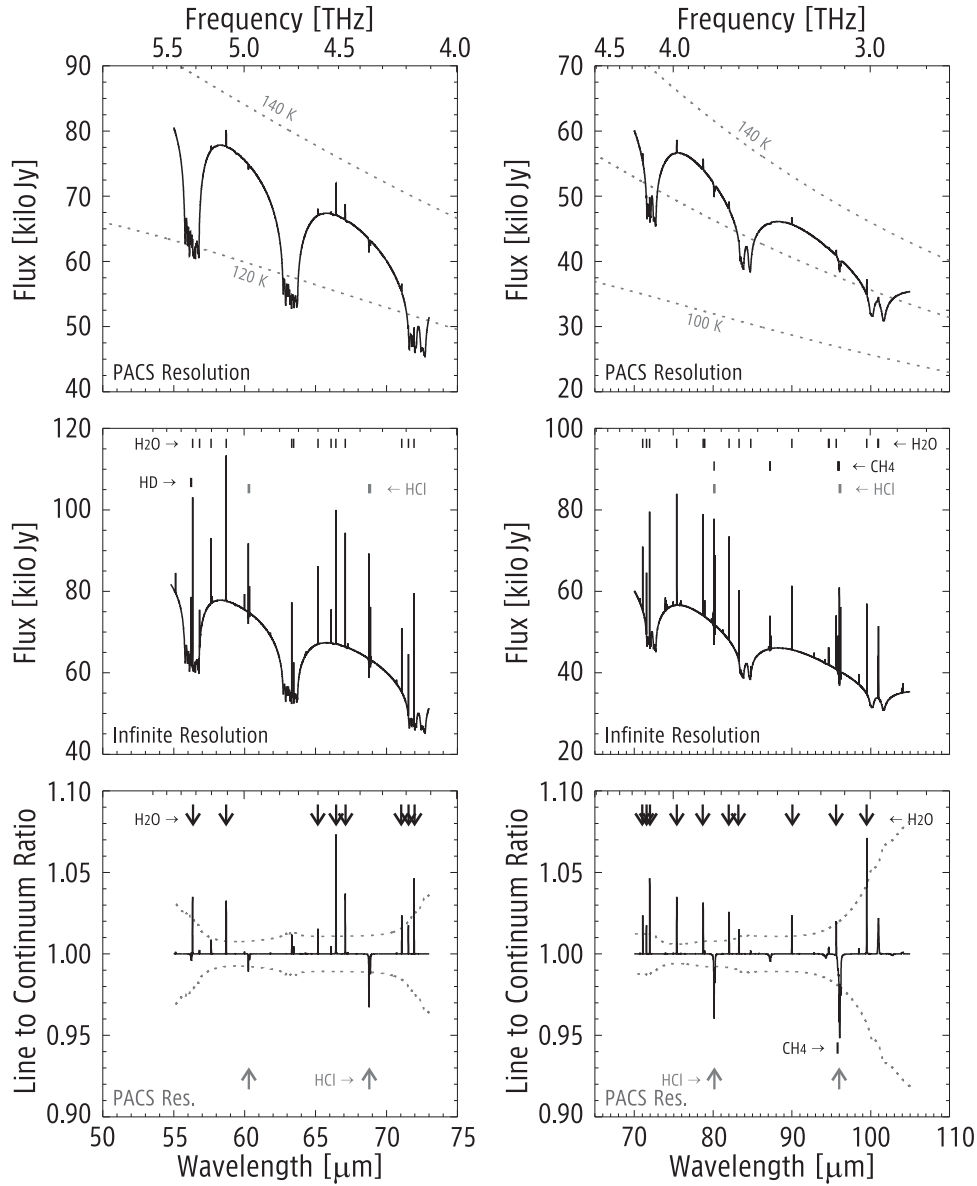


Figure 2: Synthesised full range spectrum of PACS Jupiter observation for the blue channel. Left and right columns correspond to 3<sup>rd</sup> and 2<sup>nd</sup> order of the grating, respectively. (a): The synthetic spectrum considering PACS spectral resolution. The amplitude is shown in terms of flux density for one spatial pixel. The dotted curves represent the level of flux emitted by a black body of a constant temperature (100, 120 and 140 K). (b): Infinite spectral resolution spectrum before convolution with PACS instrumental function. Small ticks show the line positions for molecules of interest. (c): The line-to-continuum ratio spectrum where the continuum emission is referenced to the H<sub>2</sub> and He collision induced absorptions and to the NH<sub>3</sub> opacity. The dotted curves represent the 5- $\sigma$  level calculated from the assumed NESR.

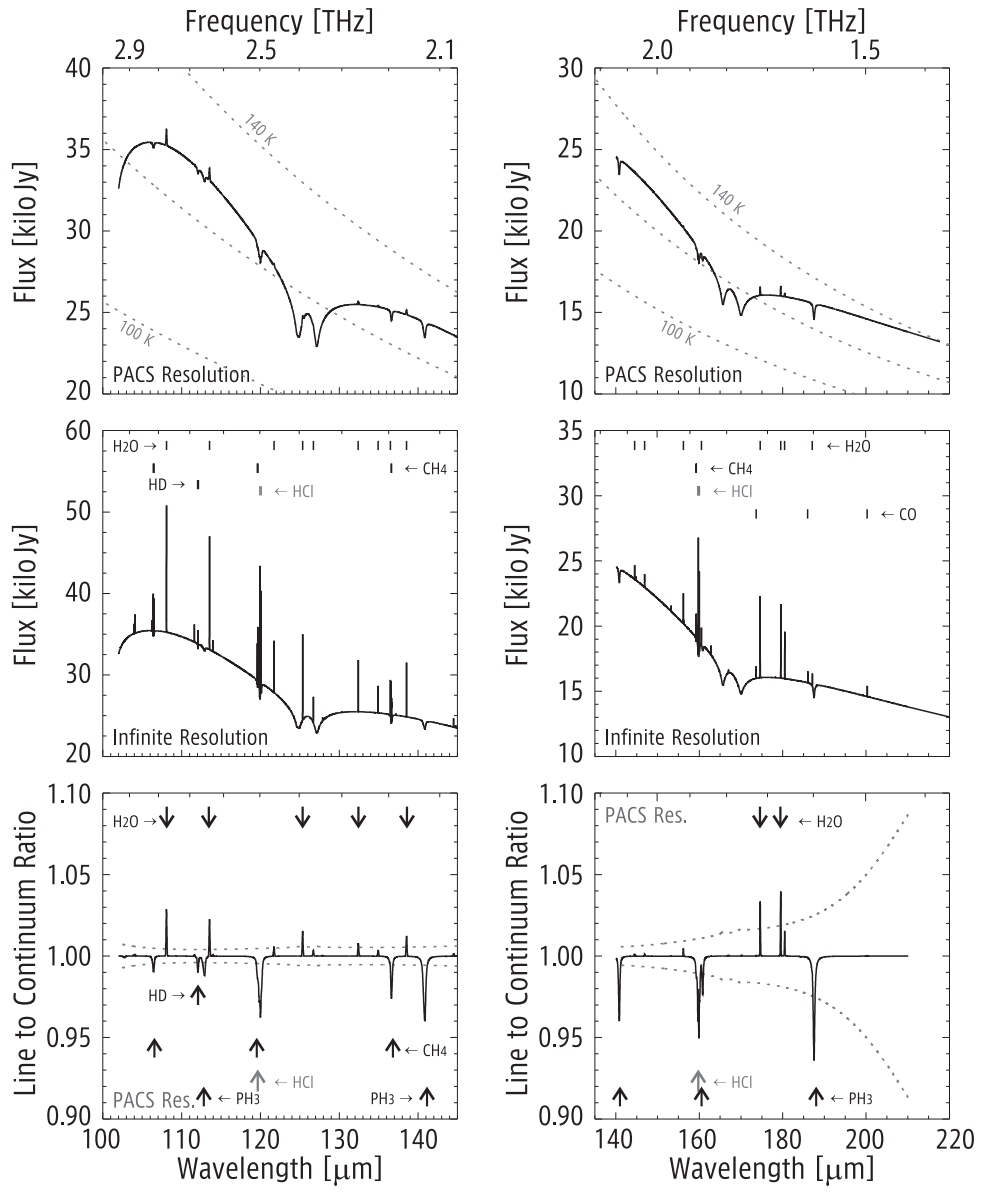


Figure 3: Same with Fig. 2, but for the red channel (1<sup>st</sup> order of the grating).

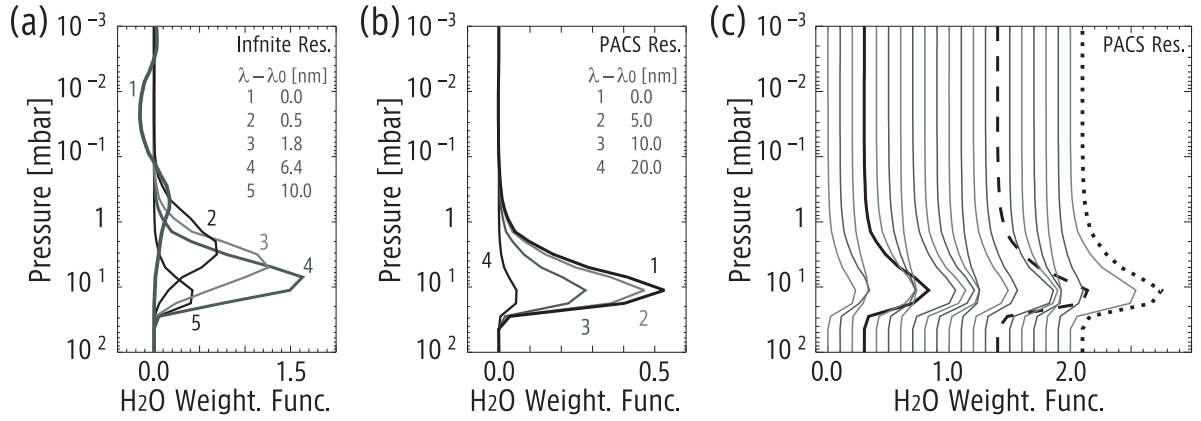


Figure 4: Weighting functions with respect to the  $\text{H}_2\text{O}$  abundance, for the  $66.4\ \mu\text{m}$  line ((a) & (b)) and for different  $\text{H}_2\text{O}$  transitions indicated by the arrows at the lowermost panels of Fig. 2–3. The panel (a) refers to the case without convolution with the PACS instrumental function, whereas the panels (b) & (c) correspond to the case with this convolution taken into account. In the panels (a) & (b), each curve represents the weighting function at different wavelength offset from the line centre. In the panel (c), each weighting function is plotted with a certain offset value, and the curves for the three highest SNR lines at  $\lambda = 66.4, 99.5$  and  $179.5\ \mu\text{m}$  are highlighted with bold, dashed and dotted lines, respectively, for clarity.

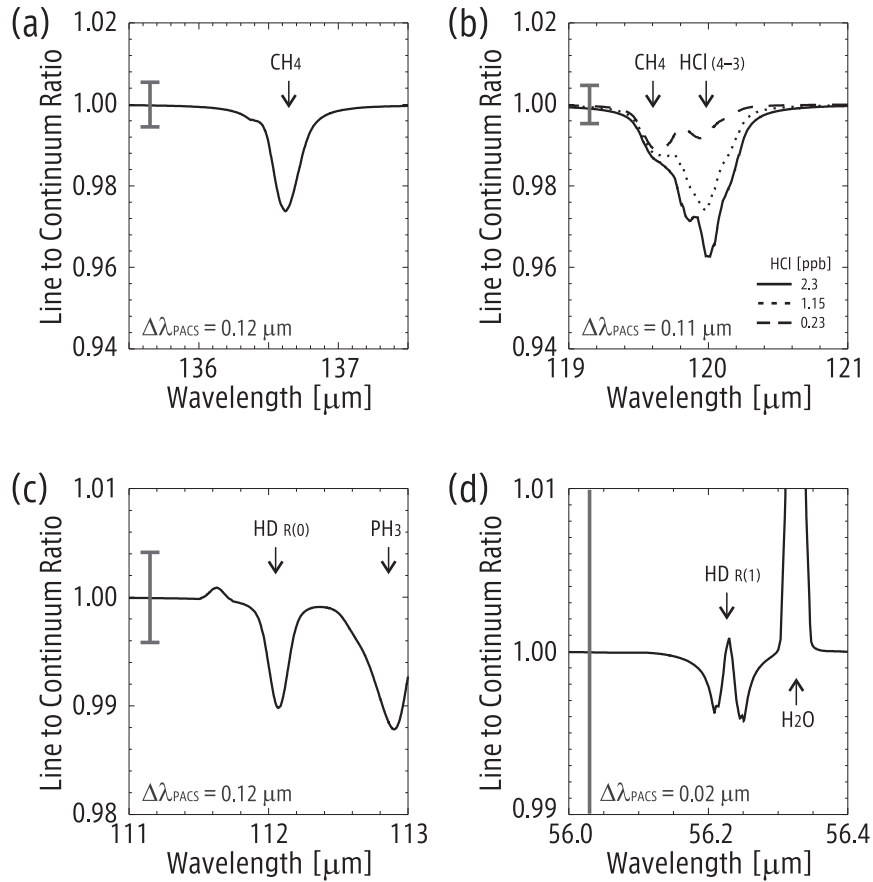


Figure 5: Simulated PACS line-to-continuum ratio spectra for the minor species. The gray bar at the left end of each spectrum indicates the  $5\text{-}\sigma$  levels of the assumed NESR. Corresponding PACS spectral resolutions are indicated inside each panel. (a): Close-up on the  $136.6\text{ }\mu\text{m}$   $\text{CH}_4$  line. (b): Close-up on the  $\text{HCl}(4\text{-}3)$  transition. The bold solid, dotted, dashed lines represent the cases of  $\text{HCl}$  abundance of 0.23, 1.15, and 2.3 ppb, respectively. (c) & (d): Close-up on the  $\text{HD}$  rotational transitions.

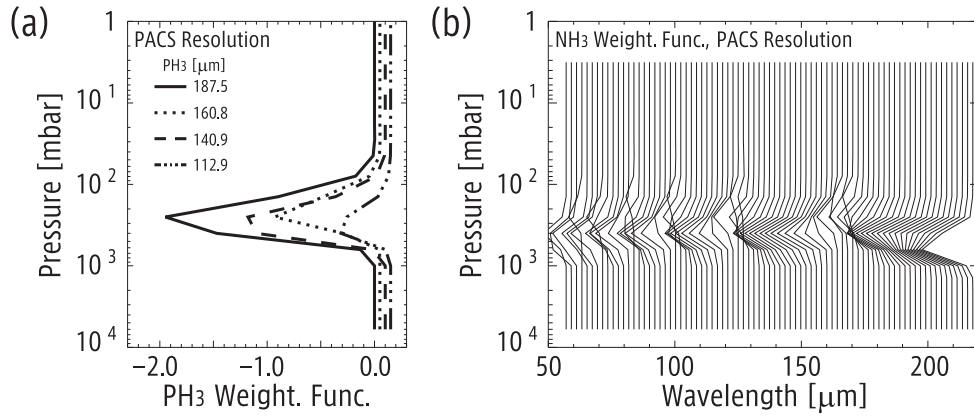


Figure 6: Weighting functions with respect to (a) PH<sub>3</sub> and (b) NH<sub>3</sub> after considering the PACS spectral resolution. For PH<sub>3</sub>, 4 lines which are indicated by the arrows at the lowermost panel of Fig. 3 are considered. For NH<sub>3</sub>, the weighting functions along the PACS spectral range are plotted.